Ultrasound-Induced Disruption of Amphiphilic Block Copolymer Micelles

Juan Xuan, Maxime Pelletier, Hesheng Xia,* Yue Zhao*

Ultrasound-induced disruption of PEO-*b*-PTHPMA, PEO-*b*-PIBMA, PEO-*b*-PTHFEMA, and PEO-*b*-PMMA block copolymer micelles in aqueous solution was investigated. Fluorescence change of loaded NR, DLS, IR, AFM, and SEM show that those micelles could be disrupted differently by 1.1 MHz high-intensity focused ultrasound beams. The micelles of PEO-*b*-PIBMA and PEO-*b*-PTHPMA appear to be more sensitive to ultrasound irradiation, resulting in a more severe micellar disruption, and IR spectra show evidence of ultrasound-induced chemical reactions, most likely hydrolysis. PEO-*b*-PMMA appear to resist HIFU irradiation better, and IR analysis found no evidence of chemical reactions. This study provides new evidence for the prospect of ultrasound-responsive BCP micelles for controlled delivery applications.

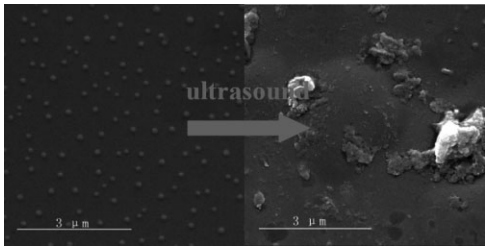

Introduction

In the research and development of stimuli-responsive block copolymer (BCP) micelles for controlled delivery applications, to date the use of ultrasound[1] as an external stimulus has been less explored than the use of pH,[2] temperature,[3] or even light.[4] And yet ultrasound may have some unique advantages over other types of stimuli, in particular with focused, high-frequency diagnostic ultrasound. In addition to possible temporal and spatial control by selecting the time of ultrasound application and the place of its action (around the focal region of the sound beams), ultrasound can easily penetrate deep in the body, in contrast with light that does have the time and location selectivity, but a limited penetration depth.[5] Generally, the disruption of BCP micelles by ultrasound is believed to originate from some thermal and solvodynamic shear effects associated with the acoustic cavitation phenomenon in solution (formation, growth, and collapse of micrometer-sized bubbles).[6] An important challenge is to develop polymer micelles that can be disrupted effectively by high-frequency, high-intensity focused ultrasound (HIFU) that is harmless to healthy cells and tissues (thus more suitable for drug delivery), but has a weaker cavitation effect than low-frequency power ultrasound. To achieve this goal, systematic investigations are required to unveil and understand the effect of BCP chemical structures on the reaction of micelles to ultrasound irradiation. This would be a first step toward rationally designed BCP micelles for HIFU-controllable micellar disruption and release of loaded guest molecules.

In a previous study,[7] we found that micelles of an amphiphilic poly(ethylene oxide)-*block*-poly(2-tetrahydropyranyl methacrylate) (PEO-*b*-PTHPMA) diblock copolymer could be disrupted by high-frequency (1.1 MHz) HIFU. The micellar disruption in aqueous solution was evidenced by the characterization results obtained with dynamic light scattering (DLS), atomic force microscopy (AFM), fluores-

J. Xuan, H. Xia
State Key Laboratory of Polymer Materials Engineering, Polymer Research Institute, Sichuan University, Chengdu 610065, China
E-mail: xiahs@scu.edu.cn
M. Pelletier, Y. Zhao
Département de chimie, Université de Sherbrooke, Sherbrooke, Québec J1K 2R1, Canada
E-mail: yue.zhao@usherbrooke.ca

DOI: 10.1002/macp.201000624

cence, and infrared (IR)–spectroscopy. Although the hypothesis of hydrolysis was supported by IR analysis,[7] the observed decrease in pH upon ultrasound expose could be a reaction of water under certain conditions.[8] As a continuing effort on ultrasound-sensitive BCP micelles, in the present work, we have synthesized three new diblock copolymers in addition to PEO-*b*-PTHPMA, which are poly(ethylene oxide)-*block*-poly[1-(isobutoxy)ethyl methacrylate] (PEO-*b*-PIBMA), poly(ethylene oxide)-*block*-poly[(2-tetrahydrofuranyloxy)ethyl methacrylate] (PEO-*b*-PTHFEMA), and poly(ethylene oxide-*block*-poly(methyl methacrylate) (PEO-*b*-PMMA). Using the four BCPs that differ in the micelle-core-forming hydrophobic polymethacrylate block, we conducted a comparative study on the disruption of their micelles by high-frequency HIFU under well-controlled conditions with no change in pH (buffer solutions at pH = 7). The chemical structures of the BCPs are shown in Figure 1, together with the acronyms and the BCP compositions as determined by ^{1}H NMR. While PTHPMA has a tetrahydropyrane ring linked to the ester group, PTHFEMA has a tetrahydrofurane ring with an ethoxy spacer, PIBMA isobuthyl ether, and PMMA a methyl group. The results reported herein show that all BCP micelles could be disrupted by high-frequency HIFU, but the extent of disruption appears to be influenced by the chemical structure of the hydrophobic block, as revealed by the characterization results.

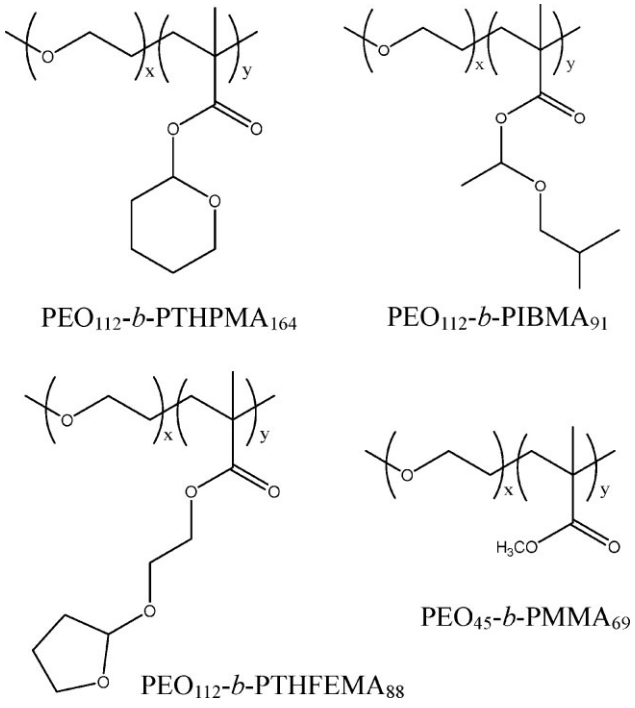

Figure 1. Chemical structures, acronyms, and compositions of the used amphiphilic block copolymers.

Experimental Part

Synthesis of Diblock Copolymers

Materials

Dichloromethane (99%) was purified by distillation from calcium hydride. All the monomers were purified by passing through a column of basic aluminum oxide before use. 2-Hydroxyethyl methacrylate (98%), 2,3-dihydrofuran (99%), isobutyl vinyl ether (99%), poly(4-vinylpyridine hydrochloride), phenothiazine, sodium carbonate anhydrous, calcium hydride, *N,N,N′,N″,N″*-pentamethyldiethylenetriamine (PMDETA, 99%), copper(I) chloride [Cu(I)Cl, 98%] were purchased from Aldrich and used without further purification. The synthesis of PEO-*b*-PTHPMA was reported previously.[9] Detailed below are the syntheses of PEO-*b*-PIBMA and PEO-*b*-PTHFEMA using atom-transfer radical polymerization (ATRP) and their respective methacrylate monomer. PEO-*b*-PMMA is a well-known block copolymer; its synthesis using ATRP will not be described here.

Synthesis of 1-(Isobutoxy)ethyl Methacrylate (IBMA)

Methacrylic acid (4.0 g, 46.5 mmol), isobutyl vinyl ether (9.3 g, 93.0 mmol), poly(4-vinylpyridine) hydrochloride (P4VP · HCl, 168 mg, 1.1 mmol), and phenothiazine (15 mg, inhibiter) were mixed in a round-bottom flask. The mixture was then heated to 70 °C overnight. The mixture was filtered to remove P4VP·HCl and phenothiazine (15 mg, inhibiter); then Na_2CO_3 (500 mg, 4.7 mmol) and CaH (500 mg, 11.9 mmol) were added carefully. After concentration in a rotary evaporator, the solution was distilled under reduced pressure at 25 °C (water bath) to give a transparent liquid (4.1 g, yield 48%).

^{1}H NMR ($CDCl_3$) δ = 6.13 (s, 1H, $-CH_2CC-$), 5.95 (q, 1H, –OCHO–), 5.56 (s, 1H, $-CH_2CC-$), 3.32 [m, 2H, $-CH_2CH(CH_3)_2-$], 1.95 (s, 3H, $-CH_3CCO-$), 1.85 [s, 1H, $-CH(CH_3)_2-$], 1.46 (d, 3H, $-CH_3CHO-$), 0.91 [d, 6H, $-(CH_3)_2CH-$].

Synthesis of (2-Tetrahydrofuranyloxy)ethyl Methacrylate (THFEMA)

2-Hydroxyethyl methacrylate (3.0 g, 23.0 mmol), 2,3-dihydrofuran (3.2 g, 45.7 mmol), P4VP·HCl (77 mg, 0.5 mmol), and phenothiazine (10 mg, inhibitor) were charged in a round-bottom flask. The solution was heated to 70 °C and stirred overnight. Afterward, the mixture was filtered to remove P4VP·HCl. Before distillation, phenothiazine (10 mg, inhibitor), Na_2CO_3 (500 mg, 4.7 mmol), and CaH (500 mg, 11.9 mmol) were added. The excess of 2,3-dihydrofuran was removed by evaporation under reduced pressure. Finally, the solution was distilled under reduced pressure at 30 °C to give a transparent liquid (4.1 g, yield 90%).

^{1}H NMR ($CDCl_3$) δ = 6.13 (s, 1H, $-CH_2CC-$), 5.56 (s, 1H, $-CH_2CC-$), 5.10 (t, 1H, –OCHO–), 4.22 (m, 2H, $-CH_2CH_2O-$), 3.85 (m, 2H, $-CH_2OCH-$), 3.60 (m, 2H, $-CH_2CH_2CH_2CH-$), 1.85 (7H, CH_3C, CH_2CH_2CH).

Synthesis of PEO-*b*-PIBMA Diblock Copolymer

The bromine end-capped PEO macroinitiator with a molecular weight of 5 000 g · mol^{-1}, designated as PEO_{112}-Br, was prepared

following a literature method.[10] IBMA (744 mg, 4.00 mmol), PMDETA (41.6 mg, 0.24 mmol), and Cu(I)Cl (11.9 mg, 0.12 mmol) were added to a solution of PEO_{112}-Br (400 mg, 0.079 mmol) dissolved in anisole (700 mg). The reaction mixture placed in a flask was degassed three times using the freeze/pump/thaw procedure. After 30 min of stirring at room temperature, it was immersed in a preheated oil bath at 50 °C for 2 h. Afterward, the mixture was passed through a neutral Al_2O_3 column with dichloromethane as eluent to remove the catalyst. The solution was concentrated upon solvent evaporation under reduced pressure and then precipitated twice in cold ether (ice bath). A white powder of the diblock copolymer (469 mg, yield 41%) was collected by filtration and dried in a vacuum oven. The reaction gave the sample PEO_{112}-*b*-$PIBMA_{91}$ whose composition was determined from the ^{1}H NMR spectrum by comparing the integrals of the resonance peaks of PEO ($\delta = 3.73$) and PIBMA ($\delta = 5.65$). ^{1}H NMR ($CDCl_3$) $\delta = 5.65$ (broad, 1H, –OCHO–), 3.73 (broad, 4H, CH_2CH_2O), 3.35 [m, 2H, $-CH_2CH(CH_3)_2-$], 1.95 [m, 1H, $-CH(CH_3)_2-$], 1.35 (broad, 3H, $-CH_3CHO-$), 0.91 [broad, 6H, $-(CH_3)_2CH-$]. $\overline{M}_n$ (^{1}H NMR) = 22 000 g · mol^{-1}, $\overline{M}_n$ (GPC) = 31 000 g · mol^{-1}, $\overline{M}_w/\overline{M}_n = 1.23$.

Synthesis of PEO-*b*-PTHFEMA Diblock Copolymer

THFEMA (856 mg, 4.00 mmol), PMDETA (41.6 mg, 0.24 mmol), and Cu(I)Cl (11.9 mg, 0.12 mmol) were added to a solution of PEO_{112}-Br (400 mg, 0.079 mmol) dissolved in anisole (800 mg). The reactive mixture placed in a flask was degassed three times using the freeze/pump/thaw procedure. After 30 min of stirring at room temperature, it was immersed in a preheated oil bath at 50 °C for 2 h. Then, the mixture was passed through a neutral Al_2O_3 column with dichloromethane as eluent to remove the catalyst. After concentration of the solution by solvent evaporation under reduced pressure, the polymer was precipitated from the dichloromethane solution in cold ether (dry ice bath), and the purification was repeated once. A white powder of diblock copolymer (376 mg, yield 30%) was collected by filtration and dried in a vacuum oven. The reaction gave the sample PEO_{112}-*b*-$PTHFEMA_{88}$, whose composition was determined from the ^{1}H NMR spectrum by comparing the integrals of the resonance peaks of PEO ($\delta = 3.73$) and PTHFEMA ($\delta = 5.10$).

^{1}H NMR ($CDCl_3$) $\delta = 5.10$ (broad, 1H, –OCHO–), 4.22 (m, 2H, $-CH_2CH_2O-$), 3.85 (m, 2H, $-CH_2OCH-$), 3.73 (broad, 4H, CH_2CH_2O), 3.60 (m, 2H, $-CH_2CH_2CH_2CH-$), 1.85 (7H, CH_3C, CH_2CH_2CH) $\overline{M}_n$ (^{1}H NMR) = 23 000 g · mol^{-1}, $\overline{M}_n$ (GPC) = 33 000 g · mol^{-1}, $\overline{M}_w/\overline{M}_n = 1.19$.

Micelle Preparation and Ultrasound Irradiation

Basically the same micelle preparation and ultrasound irradiation procedures as in the previous report[7] were utilized in the present work. Precaution was taken to ensure that micelles of the four BCPs [with or without loaded nile red (NR)] were prepared and subjected to ultrasound irradiation under exactly the same conditions. To separate the possible effect of a pH change on the micellar disruption (hydrolysis at acidic pH, for instance) from the ultrasound action, comparisons of all the BCPs were made using their micelles in buffer solutions at pH = 7. For micelle preparation, briefly, a BCP sample (3.0 mg) was dissolved in tetrahydrofuran (THF, 4.6 mL) before water was added first slowly (1.2 mL) and then quickly (1.0 mL) to induce micelle formation. The micellar solution was then diluted by water and after removal of THF by evaporation at 45 °C for 24 h, an initial polymer concentration of 0.15 mg/mL was obtained. To load NR in the micelles, which is a model hydrophobic compound, the same procedure was used except that the THF solution contained both dissolved BCP and the hydrophobic dye (0.1 mg · mL^{-1}); upon addition of water, the aggregation of the hydrophobic block allowed some NR molecules to be solubilized by polymer chains forming the core of micelle. During the removal of THF, unloaded NR was precipitated in aqueous solution and removed by filtration using a 0.22 μm membrane.

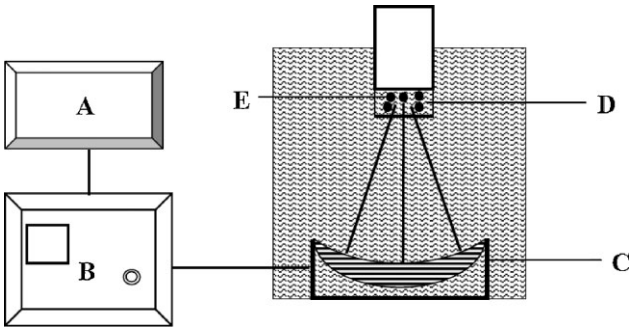

Figure 2. Experimental setup with a schematic diagram of the high-frequency HIFU apparatus: arbitrary waveform generator (A), radio-frequency power amplifier (B), acoustic lens transducer (C), water bath (D), and polymer micelles (E).

In the present study, high-frequency HIFU irradiation was generated by a commercially available ultrasound apparatus that comprises three main components: an arbitrary waveform generator (Agilent 33220A Function Generator), a radiofrequency power amplifier (A150, Electronics & Innovation), and an acoustic lens transducer (H-101, Sonic Concept, USA). As schematized in Figure 2, the acoustic lens transducer could generate focused ultrasound beams of adjustable power (up to 100 W) at a high frequency (1.1 MHz). The focal spot has a circular diameter of ≈ 1.26 mm and a height of ≈ 11 mm, and the focal length is about 63 mm. In all ultrasound irradiation experiments, the focal spot of the beams was set at the center of the micellar solution (5 mL) placed in a tube reactor immersed in a water tank, unless otherwise stated. After a certain time of ultrasound irradiation, the tube reactor was removed from the water tank and the micellar solution was used for characterizations at room temperature, the irradiation time being cumulative. We mention here that based on change in fluorescence of loaded NR, this ultrasound system is more efficient than a home-built apparatus utilized in our previous work,[7] allowing the use of smaller ultrasound powers in the present study.

Characterizations

The fluorescence of NR entrapped in BCP micelles was used to probe the ultrasound-induced micellar disruption as it is sensitive to the polarity of the environment in which the dye is located.[11] For these measurements, a fluorescence spectrophotometer (970CRT, Shanghai Precision & Scientific Instrument) was used, with the excitation wavelength set at 540 nm. Unless otherwise stated, excitation and

emission slit were set to 5 and 10 nm, respectively. Direct evidence for perturbation of BCP micelles in solution could be obtained by using dynamic light scattering (DLS) that measures the average hydrodynamic diameter (D_H) and the size distribution of micellar aggregates, as well as the scattering intensity. DLS measurements were performed on a Brookhaven BI-200 goniometer with vertically polarized incident light of wavelength $\lambda = 532$ nm supplied by an argon laser operating at 400 mW, and a Brookhaven BI-9000 digital autocorrelator. All measurements were carried out at 25 °C at a scattering angle of 90°, with the autocorrelation functions analyzed by using the non-negatively constrained least square algorithm. Unless otherwise stated, only the initial micellar solution prior to ultrasound irradiation was microfiltered through a 0.22 μm membrane. Using a Nicolet 560 Fourier-transform infrared (FTIR) spectrometer, infrared spectra of the samples prepared from ultrasound-irradiated micellar solutions were recorded at room temperature. To prepare the samples used for the infrared analysis, micellar solutions after ultrasound irradiation were first dried under vacuum at 40 °C to remove water, then redissolved in THF and finally cast on a KBr window and dried. Moreover, atomic force microscopy (AFM, NanoScope MultiMode IIIa) and scanning electron microscopy (SEM, Inspect F, Philips) were used to observe the micellar aggregates in dried state. The samples were obtained by casting a drop of the micellar solution on clean mica, followed by drying.

Results and Discussion

The formation of micelles by the four amphiphilic BCPs under the same preparation conditions was first examined. Figure 3 shows the intensity-averaged size distributions for all samples in aqueous solution as measured by DLS. Though they all self-assemble into micellar aggregates, their average sizes and size distributions are different. Of them, PEO-*b*-PMMA form small micelles with average $D_H \approx$ 28 nm, while the three others give rise to micellar aggregates of larger sizes in the range of 40–50 nm, with PEO-*b*-PTHFEMA exhibiting a much wider distribution of D_H than the other BCPs. This observation is not surprising, since these BCPs have different hydrophobic blocks, and thus different amphiphilicity with respect to the PEO block. The shorter PEO block for the PEO-*b*-PMMA sample may also account for the smaller micelles.

NR solubilized by BCP micelles emits fluorescence whose change can be used as a probe to detect micellar disruption.[11] For micelles in aqueous solution, a quenching of fluorescence can be observed if NR is released or exposed to water, in which it is insoluble and can aggregate, as a result of stimuli-induced dissociation or swelling of micelles.[9,11] Before using the fluorescence of NR to monitor ultrasound-induced disruption of BCP micelles, we performed control tests to make sure that under the used experimental conditions, the high-frequency HIFU causes no degradation of NR resulting in decrease of its fluorescence intensity. Figure 4 shows the result obtained by dissolving NR in THF. Only a slight fluorescence decrease can be noticed after 5 or 10 min irradiation at an ultrasound power of 40 W, suggesting that the used ultrasound beams could not degrade seriously NR in solution. By contrast, significant changes were observed for NR-loaded micellar solutions of the four BCPs subjected to high-frequency HIFU at a power of 40 W. Figure 5 shows their fluorescence emission spectra recorded at different ultrasound irradiation times. In all cases, the intensity decreases with increasing the cumulative irradiation time. Considering the result of the control test in Figure 4, the large decrease in the fluorescence intensity of NR should be the consequence of BCP micellar disruption by the ultrasound, bringing an increased amount of NR into contact with water that quenches the fluorescence of the dye. On the other hand, the

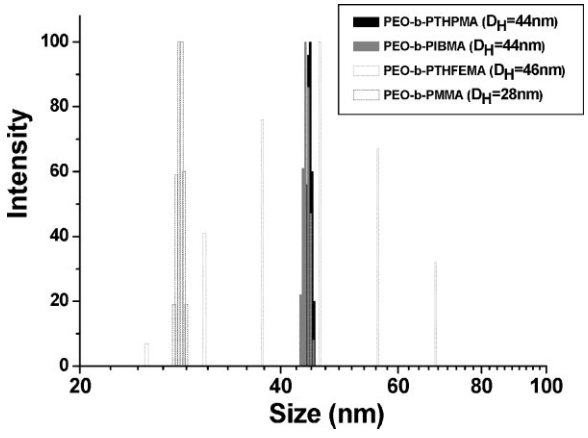

Figure 3. Size distributions of different BCP micelles in aqueous solution as revealed by DLS (the average hydrodynamic diameters are indicated in the figure).

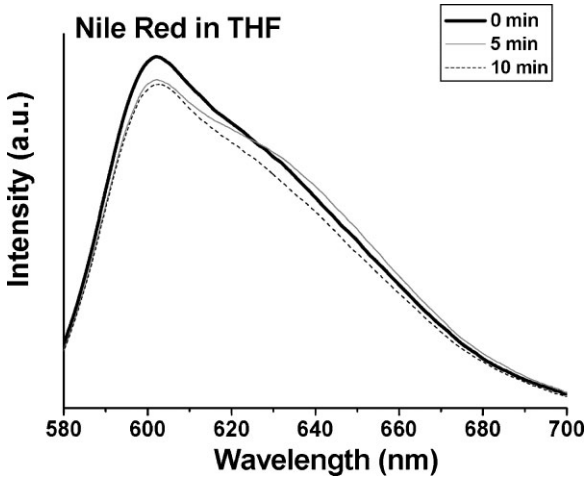

Figure 4. Fluorescence emission spectra of NR dissolved in THF (excitation: 540 nm) recorded before (0 min) and after exposure to ultrasound irradiation (5 and 10 min) (ultrasound power: 40 W, solution volume: 5 mL).

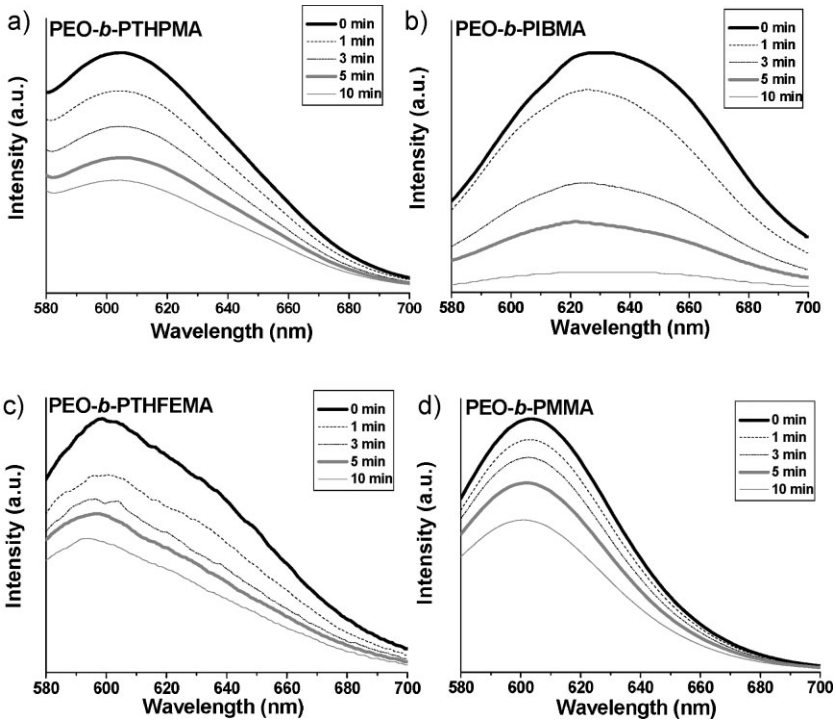

Figure 5. Fluorescence emission spectra of NR-loaded BCP micelles (excitation: 540 nm) recorded at different ultrasound irradiation times for (a) PEO-*b*-PTHPMA, (b) PEO-*b*-PIBMA, (c) PEO-*b*-PTHFEMA, and (d) PEO-*b*-PMMA, all experiments being carried out under the same conditions (ultrasound power: 40 W, micellar solution volume: 5 mL).

emission spectra of NR loaded in the four BCP micelles display different shapes and emission maximums, which reflect different polarities of the micelle cores sensed by NR molecules.

To better compare the kinetics of apparent release of NR with different BCPs, Figure 6 shows the normalized emission intensity (measured at their respective emission maximum) versus ultrasound irradiation time. It is seen that PEO-*b*-PIBMA displays the fastest NR fluorescence decrease than the others, presumably due to a greater disruption of micelles in response to ultrasound waves; whereas the change rate with micelles of PEO-*b*-PMMA is the slowest. These results show that all the BCP micelles, having a polymethacrylate core, could be more or less disrupted by ultrasound irradiation. The chemical structure of the hydrophobic micelle-core-forming polymer appears to affect the extent of disruption and the rate of the apparent release of NR. A qualitative assessment of the NR loading capacity by the four BCP micelles is worth being mentioned. Under the same preparation conditions, and based on the fluorescence intensity, PEO-*b*-PMMA appears to solubilize the most of NR, which is followed by, in the decreasing order, PEO-*b*-PTHFEMA, PEO-*b*-PIBMA, and PEO-*b*-PTHPMA.

The disruption of the BCP micelles by ultrasound was confirmed by DLS, AFM, and SEM. Figure 7 shows the DLS results of all BCP micellar solutions subjected to ultrasound irradiation (40 W). Although no clear common trend for the evolution of size distribution over irradiation time can be observed, it is clear that ultrasound could disrupt the initial BCP micelles quickly in all the solutions, and that disrupted micelles become less stable in aqueous solution and coalesce into larger aggregates. In all cases except PEO-*b*-PMMA, 1 min HIFU irradiation is enough to change quite drastically the sizes of the aggregates, with apparently the formation of larger aggregates than the initial ones and an increased polydispersity (Figure 7a–c). As the irradiation went on, their sizes undergo a continuous change, with, in some cases, the appearance of some smaller aggregates. The micelles of PEO-*b*-PMMA seem to be more resistant to ultrasound; larger aggregates were formed only after irradiation longer than 3 min (Figure 7d). By plotting the average D_H versus irradiation time, the differences between the four BCPs become clear. Much larger aggregates are formed upon ultrasound exposure for BCP solutions of PEO-*b*-PTHFEMA and PEO-*b*-PIBMA than with PEO-*b*-PTHPMA and PEO-*b*-PMMA (Figure 7e). For the former two BCPs, the average size of their aggregates increases first over the first 3–5 min of irradiation, before decreasing at longer times. The changes in light scattering intensity (measured at 90°) essentially echo the changes in the average size of the

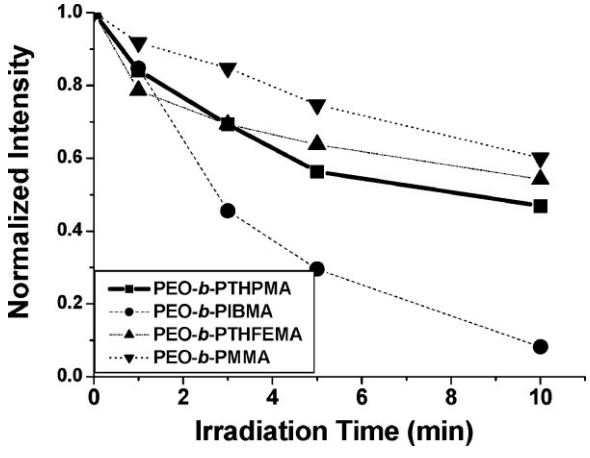

Figure 6. Normalized fluorescence emission intensity of NR versus ultrasound irradiation time for various BCP micellar solutions, using data in Figure 5 with the intensity measured at the respective emission maximum of each BCP.

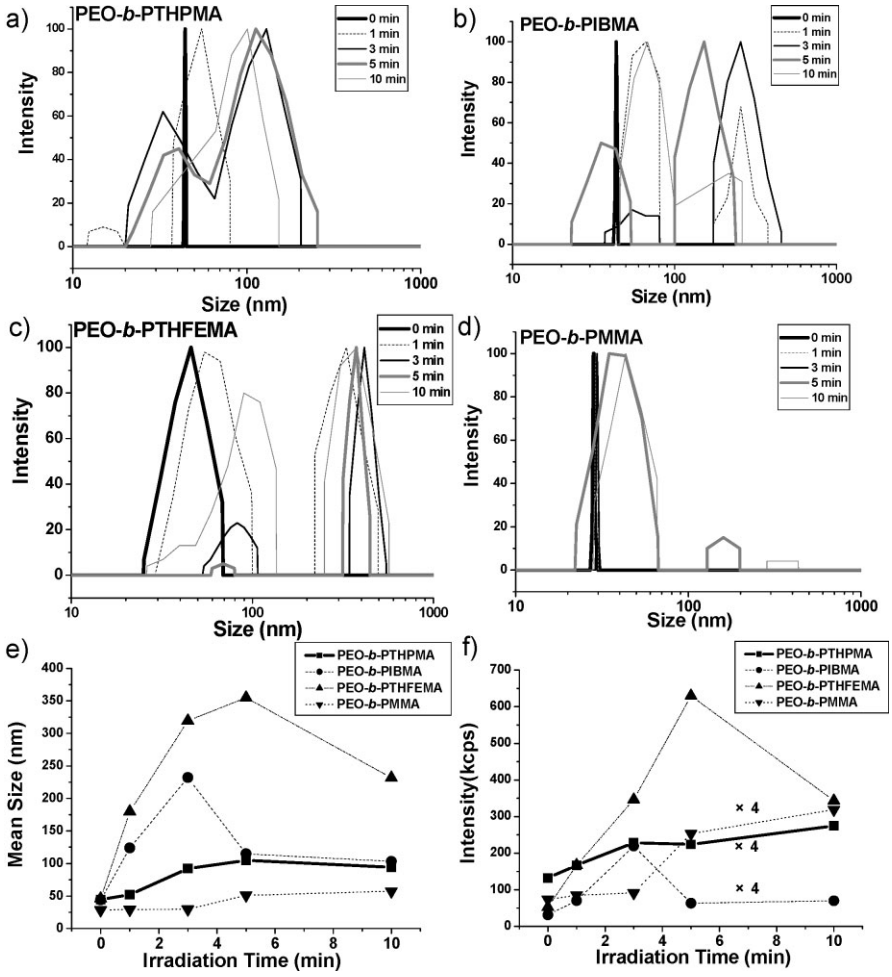

Figure 7. (a–d) Evolution of size distribution over ultrasound irradiation time for micellar aggregates of PEO-*b*-PTHPMA (a), PEO-*b*-PIBMA (b), PEO-*b*-PTHFEMA (c), and PEO-*b*-PMMA (d). (e) Mean hydrodynamic diameter (D_H) versus ultrasound irradiation time, and (f) light scattering intensity (measured at 90°) versus ultrasound irradiation time for various BCP micellar solutions. All experiments were carried out under the same conditions (ultrasound power: 40 W, micellar solution volume: 5 mL).

aggregates (Figure 7f). It is interesting to notice that the less ultrasound-sensitive micelles of PEO-*b*-PMMA show no significant size change within the first 3 min of irradiation, which corroborates with the slower ultrasound-induced fluorescence change of NR (Figure 6). Figure 8 shows an example of AFM and SEM images obtained with the micellar solution of PEO-*b*-PIBMA before and after ultrasound irradiation (10 min, 40 W). Being consistent with the DLS results, larger aggregates were formed upon irradiation, which coexist with a certain amount of smaller micelles. The SEM images are particularly clear; small micelles quite uniform in size prior to ultrasound exposure are replaced by irregular large aggregates after the irradiation.

In order to get some insight into the origin of the micellar disruption and related structural changes, infrared spectra of all BCP micelles were recorded before and after their ultrasound treatment in solution (10 min, 40 W). In this experiment, BCP micelles were prepared under the same conditions as described above, but the solutions contained no NR and were not treated with buffer in order to avoid spectral complications. The obtained spectra in the 800—1 800 cm^{-1} region are shown in Figure 9. Although a specific analysis is difficult, some observations can be made. Firstly, the spectral changes indicate the occurrence of ultrasound-induced chemical reactions, particularly with micelles of PEO-*b*-PIBMA and PEO-*b*-PTHPMA. These two BCPs display much more prominent spectral changes induced by ultrasound exposure than PEO-*b*-PTHFEMA and PEO-*b*-PMMA, which, again, is consistent with the observed differences in the fluorescence change rate of NR upon ultrasound irradiation (Figure 6). Secondly, prominent spectral changes occur in the 1 400—1 800 cm^{-1} region; for PEO-*b*-PTHPMA, the characteristic carbonyl stretch band at ≈1 735 cm^{-1} is replaced by a broad band peaked at ≈1 650 cm^{-1} after ultrasound irradiation, while PEO-*b*-

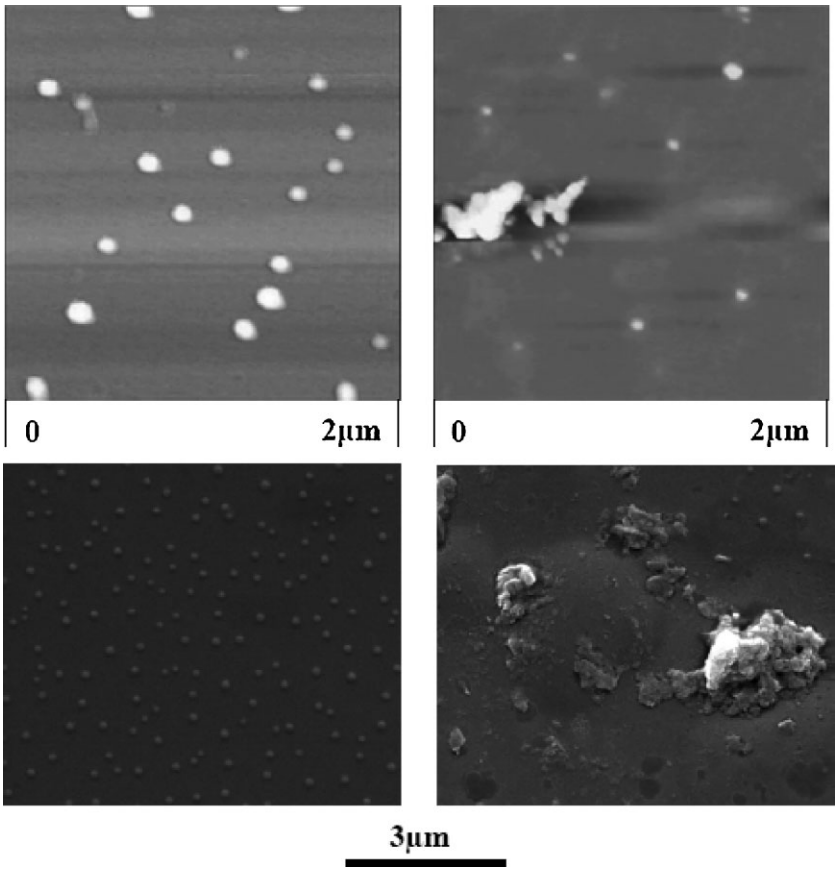

Figure 8. Images of AFM (upper) and SEM (lower) showing micelles of PEO-*b*-PIBMA before ultrasound (left) and large aggregates formed from disrupted micelles after ultrasound irradiation (right).

PIBMA displays a shift of about 15 cm^{-1} to lower wavenumbers. This spectral change is likely due to the formation of some carboxylic acid groups whose hydrogen-bonded dimers are known to absorb at lower wavenumbers.[12] Should ultrasound induce cleavage of side groups, some of generated small molecules may be removed during the thermal treatment of the sample at 40 °C in vacuum, which can also contribute to the spectra changes. Thirdly, while PEO-*b*-PMMA exhibits the smallest spectral changes among the four BCPs, PEO-*b*-PTHFEMA shows a more intense absorption band around 1 600 cm^{-1} after ultrasound irradiation.

Of the four BCPs, the micelle-core-forming hydrophobic PTHPMA, PIBMA, and PTHFEMA have a labile acetal unit in their side group, and among them, PTHPMA and PIBMA indeed are much less stable and more likely to undergo a hydrolysis reaction. The above characterization results point out that micelles based on PTHPMA- and PIBMA-containing BCPs respond more importantly to high-frequency HIFU irradiation. By contrast, PMMA is the hydrophobic block used that is less likely to have a hydrolysis reaction and, indeed, micelles of PEO-*b*-PMMA appear to be less sensitive to ultrasound. Therefore, the whole of the results of this comparative study show that the chemical structure of the hydrophobic, micelle-core-forming polymethacrylate could influence greatly the extent of ultrasound-induced disruption of BCP micelles. It appears that with ester groups more likely to undergo hydrolysis reaction, high-frequency HIFU irradiation could induce more significant chemical reactions, most likely hydrolysis, which leads to a more severe micellar disruption. We mention that under the used ultrasound irradiation conditions (power and time), the temperature of the aqueous solution in the tube reactor is around 30 °C. No thermally induced hydrolysis of the BCP could occur in this range of temperatures. Of course, there may also be differences in terms of ultrasound-induced physical disruption for micelles of BCPs of different chemical structures. It is easy to imagine that for a micelle core that is softer, i.e., less compact or rigid, it should be more probable to be perturbed by any mechanical shearing effect associated with the ultrasound. The observed micellar disruption should be the overall result of the chemical and physical disruption effects exerted on the micelles by ultrasound waves. At this time, we are unable to assess separately their respective role in the process. One difficulty is the very small amount of polymers involved in this type of experiments, which prevents the use of such methods as size exclusion chromatograph and HPLC to detect possible chain scission or to further identify new chemical species after ultrasound irradiation. We note that more thorough and quantitative characterizations will be targeted in a future work, which is out of the scope of the present study.

An important potential advantage of ultrasound-based release is that it may have a temporal and spatial selectivity similar to the use of light-controllable nanovectors, while affording a much greater tissue penetration depth than light. The spatial selectivity can be enhanced if the ultrasound-induced disruption of micelles takes place predominantly around the focal area of the beams. We conducted the experiment described in Figure 10 to evaluate this aspect. Using NR-loaded micellar solutions of PEO-*b*-PIBMA and PEO-*b*-PTHPMA, the apparent release of NR, monitored by the change in fluorescence emission,

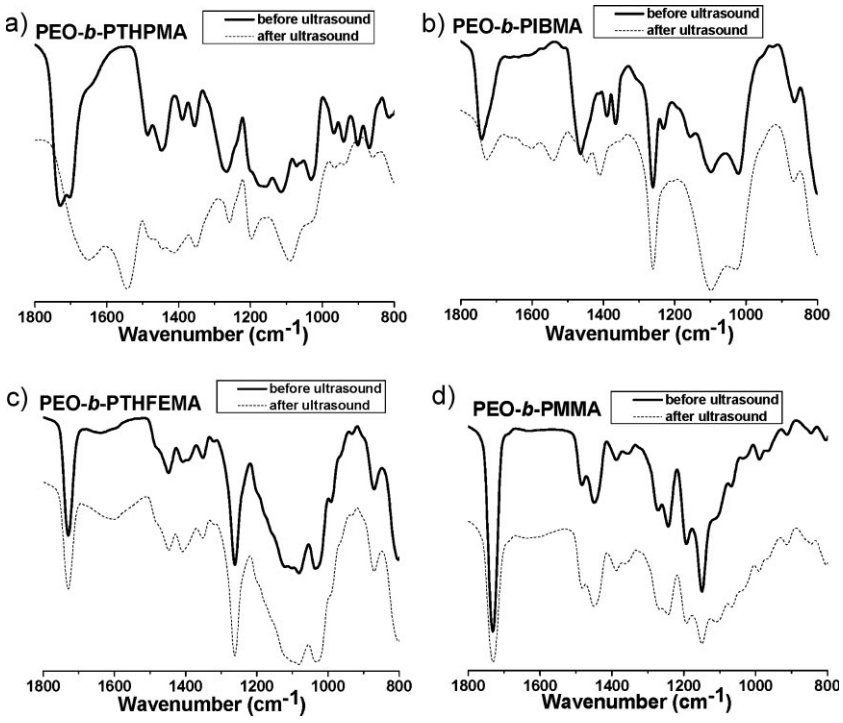

Figure 9. Infrared spectra of solid samples obtained from various BCP micelles before and after ultrasound irradiation (10 min, ultrasound power 40 W).

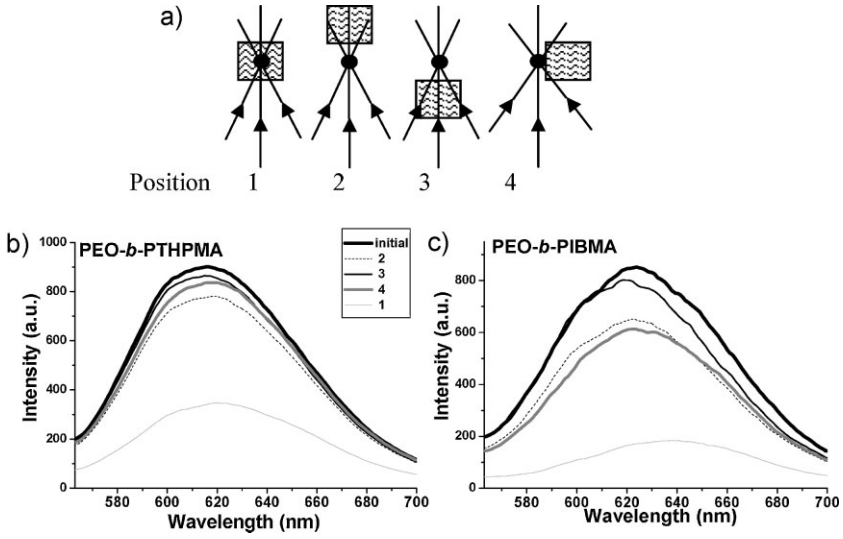

Figure 10. (a) Schematic of different positions of the focal spot of ultrasound beams with respect to micellar solution. (b) and (c) Fluorescence emission spectra of NR (excitation 540 nm) recorded after 5 min ultrasound irradiation (40 W) with different focal spot positions for micelles of PEO-*b*-PTHPMA (b) and PEO-*b*-PIBMA (c).

was allowed to occur under exactly the same conditions except the position of the focal spot of the ultrasound beams with respect to the solution. As depicted in Figure 10a, the focal point was placed right in the middle of the solution (position 1), above and beneath the center of solution by 2 cm (positions 2 and 3) and at the level of the solution center but just outside a wall of the tube reactor (position 4). With both PEO-*b*-PIBMA (Figure 10b) and PEO-*b*-PTHPMA (Figure 10c), it is seen that the release of NR was much more important with position 1 than with positions 2–4, for which the solution was subjected to non-focused (or less focused) ultrasound beams. These results indicate that ultrasound-induced micellar disruption is more severe under focused beams, which makes it possible to choose the place of action by controlling the location of the focal spot of ultrasound beams. Finally, Figure 11 shows two examples of results that show the effect of ultrasound power (beam intensity) on the fluorescence change rate of NR. With both micelles of PEO-*b*-PTHPMA (Figure 11a) and PEO-*b*-PIBMA (Figure 11b), it is no surprise to find out that the release becomes faster with increasing the power. This clearly is the result of a faster and more severe disruption of BCP micelles by a more powerful ultrasound irradiation. At a power output of 100 W, 5 min exposure to high-frequency HIFU is enough to quench almost completely the fluorescence of NR. Actually, with this high power, the shift of fluorescence emission maximum to ≈640 nm indicates that most dye molecules are in an aqueous medium. In addition to irradiation time, adjusting the ultrasound power is another way to control the extent of micellar disruption and the concomitant release of encapsulated molecules. As more NR molecules are brought into water by ultrasound, the color of the micellar solution due to absorption of encapsulated dye molecules becomes increasingly faded (pictures not shown).

Conclusion

We conducted a comparative study on the disruption of BCP micelles and the concomitant release of encapsulated NR molecules by high-frequency HIFU irradiation. We found that all micelles formed by the four BCPs composed of a PEO hydrophilic block and a different polymethacrylate hydrophobic block could be disrupted by ultrasound resulting in release of NR. However, the extent of micellar disruption and release was

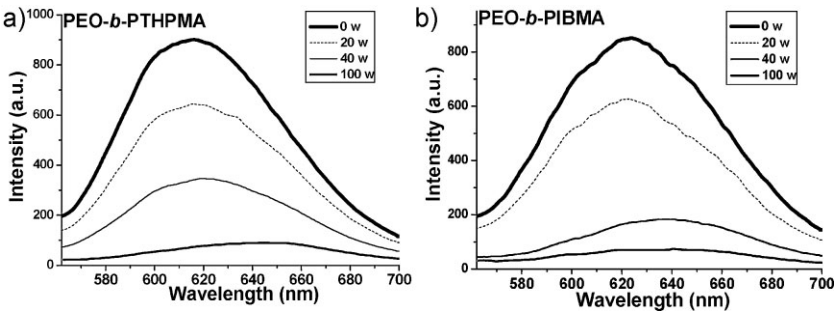

Figure 11. Fluorescence emission spectra of NR-loaded BCP micelles (excitation 540 nm) recorded after 5 min ultrasound irradiation with different powers for PEO-*b*-PTHPMA (a) and PEO-*b*-PIBMA (b).

found to be influenced by the chemical structure of the micelle-core-forming hydrophobic polymethacrylate. On the one hand, micelles of PEO-*b*-PIBMA and PEO-*b*-PTHPMA, whose hydrophobic blocks have a labile acetal unit in the side group and are more likely to undergo ester hydrolysis, could be disrupted more severely by ultrasound, giving rise to a faster release of NR. On the other hand, micelles of PEO-*b*-PMMA, whose polymethacrylate block is more stable, appear to be more resistant to ultrasound and exhibit a slower rate of release of NR than other BCPs. Moreover, infrared spectra recorded with micelles before and after ultrasound irradiation of their aqueous solution show evidence for the occurrence of chemical reactions, most likely hydrolysis, for PEO-*b*-PIBMA and PEO-*b*-PTHPMA, but absence of chemical reactions for PEO-*b*-PMMA. The effect of BCP chemical structure on the reaction of micelles to high-frequency UIFU irradiation, as evidenced by the present study, shows the perspective of designing and developing ultrasound-sensitive BCP micelles for ultrasound-based delivery applications.

Acknowledgements: This study was funded by *National Natural Science Foundation (NSFC) of China* (Grant No: 51073100). H. X. also acknowledges support from the *Program for New Century Excellent Talents in Universities, China*. Y. Z. acknowledges financial support from the *Natural Sciences and Engineering Research Council of Canada* (NSERC) and *Le Fonds québecois de la recherche sur la nature et les technologies of Quebec (FQRNT)*. We are grateful to *St-Jean Photochemicals Inc.* (St-Jean-sur-Richelieu, Quebec, Canada) for providing us with the monomer of tetrahydropyranyl methacrylate. We also thank Prof. *Yves Dory (University of Sherbrooke)* for helpful discussions.

Received: October 8, 2010; Revised: November 16, 2010; Published online: January 12, 2011; DOI: 10.1002/macp.201000624

Keywords: block copolymers; micelles; stimuli-sensitive polymers; ultrasound

[1] [1a] N. Y. Rapoport, *Colloids Surf. B: Biointerfaces* **1999**, *16*, 93; [1b] G. A. Husseini, G. Myrup, W. G. Pitt, D. A. Christensen, N. Y. Rapoport, *J. Controlled Release* **2000**, *69*, 43; [1c] A. Marin, H. Sun, G. A. Husseini, W. G. Pitt, D. A. Christensen, N. Y. Rapoport, *J. Controlled Release* **2002**, *84*, 39.

[2] See for example, [2a] E. R. Gillies, J. M. J. Frechet, *Chem. Commun.* **2003**, 1640; [2b] E. G. Bellomo, M. D. Wyrsta, L. Pakstis, D. J. Pochan, T. J. Deming, *Nat. Mater.* **2004**, *3*, 244; [2c] Y. Bae, S. Fukushima, A. Harada, K. Kataoka, *Angew. Chem. Int. Ed.* **2003**, *42*, 4640; [2d] X. Xu, A. E. Smith, S. E. Kirkland, C. L. McCormick, *Macromolecules* **2008**, *41*, 8429; [2e] X. Jiang, B. Zhao, *Macromolecules* **2008**, *41*, 9366.

[3] See, for example, [3a] J. E. Chung, M. Yokoyama, T. Okano, *J. Controlled Release* **2000**, *65*, 93; [3b] C. M. Schilli, M. Zhang, E. Rizzardo, S. H. Thang, Y. K. Chong, K. Edwards, G. Karlsson, H. E. Muller, *Macromolecules* **2004**, *37*, 7861; [3c] S. Qin, Y. Geng, D. E. Discher, S. Yang, *Adv. Mater.* **2006**, *18*, 2905; [3d] J. Rodriguez-Hernandez, F. Checot, Y. Gnanou, S. Lecommandoux, *Prog. Polym. Sci.* **2005**, *30*, 712.

[4] [4a] Y. Zhao, *J. Mater. Chem.* **2009**, *19*, 4887; [4b] Y. Wang, H. Xu, X. Zhang, *Adv. Mater.* **2009**, *21*, 2849; [4c] G. Wang, X. Tong, Y. Zhao, *Macromolecules* **2004**, *37*, 8911; [4d] J. Jiang, X. Tong, Y. Zhao, *J. Am. Chem. Soc.* **2005**, *127*, 8290; [4e] J. Babin, M. Pelletier, M. Lepage, J. F. Allard, D. Morris, Y. Zhao, *Angew. Chem. Int. Ed.* **2009**, *48*, 3329.

[5] [5a] W. G. Pitt, G. A. Husseini, B. Staples, *J. Expert Opin. Drug Delivery* **2004**, *1*, 37; [5b] J. Kost, K. Leong, R. Langer, *Proc. Natl. Acad. Sci. U. S. A* **1989**, *86*, 7663; [5c] J. E. Kennedy, *Nat. Rev. Cancer* **2005**, *5*, 321.

[6] [6a] K. S. Suslick, *Science* **1990**, *3*, 1439; [6b] C. P. Zhu, S. C. He, M. L. Shan, J. C. Chen, *Ultrasonics* **2006**, *44*, e349; [6c] C. R. Thomas, C. H. Farny, C. C. Coussios, R. A. Roy, *Acoust. Res. Lett.* **2005**, *6*, 182.

[7] J. Wang, M. Pelletier, H. Zhang, H. Xia, Y. Zhao, *Langmuir* **2009**, *25*, 13201.

[8] K. Shinobu, E. Kenji, K. Yoshihiro, N. Hiroyasu, K. Kogaku, *Ronbunshu* **1999**, *25*, 290.

[9] M. Pelletier, B. Jerome, L. Tremblay, Y. Zhao, *Langmuir* **2008**, *24*, 12664.

[10] Y. Tian, K. Watanabe, X. Kong, J. Abe, T. Iyoda, *Macromolecules* **2002**, *35*, 3739.

[11] A. P. Goodwin, J. L. Mynar, Y. Ma, G. R. Fleming, J. M. J. Frechet, *J. Am. Chem. Soc.* **2005**, *127*, 9952.

[12] J. Dong, Y. Ozaki, K. Nakashima, *Macromolecules* **1997**, *30*, 1111.